A statistical model and simulator for cardiovascular pressure signals

C Staats, D Austin*, and **M Aboy**
Electrical Engineering Department, Oregon Institute of Technology, Beaverton, OR, USA

The manuscript was received on 26 July 2007 and was accepted after revision for publication on 11 March 2008.

DOI: 10.1243/09544119JEIM348

Abstract: Physiological signal simulators are often used to conduct validation studies of commercially available devices such as oscillometric non-invasive blood pressure (NIBP) monitors. Numerous assessment studies have been conducted using simulators to validate commercial NIBP monitors. While there are several simulators commercially available to evaluate oscillometric NIBP devices, currently there are no simulators designed to validate invasive pressure signal devices.

A statistical model and simulator for invasive cardiovascular pressure signals such as arterial blood pressure and intracranial pressure are described. The model incorporates the effects of respiration on pressure signals and can be used to generate synthetic signals with time and frequency domain characteristics matching any desired subject population. Additionally, the way that noise and artefacts typically present in real pressure signals should be modelled is described. The proposed statistical model is a useful tool for validation of algorithms designed to process or analyse biomedical pressure signals to estimate parameters of clinical interest such as the cardiac frequency, heart rate variability, respiratory frequency, and pulse pressure variation in the presence of noise. The model can be used to simulate signals in order to validate commercial devices that process and analyse invasive pressure signals.

Keywords: arterial blood pressure, intracranial pressure, simulators, non-invasive blood pressure simulators

1 INTRODUCTION

Biomedical signal models are important tools for research, development, comparison, and validation of algorithms that operate on physiological signals [**1**]. This is because most algorithms cannot be tested directly on data as the parameter of interest is not directly measurable [**2**]. As a result of the inability to use patient data for validation or development, many models have been utilized. Models as simple as adding noise to pre-recorded patient data for the verification of bispectrum averaging in waveform estimation [**3**] to those as complex as generating synthetic binary spike trains for tremor frequency tracking validation [**4**] have been extensively used in research. In reference [**5**], a model was developed to validate a stationary segmentation algorithm for extracellular microelectrode recordings. Models of the electromyogram (EMG) have also been proposed for such purposes as model-based signal interpretation [**6**], analysis of the sources of cross-talk [**7**], investigation of the contribution of amplitude and frequency spectrum from motor units in surface EMG [**8**], and exploration of the effect of limb geometry on surface-detected muscle fibre action potentials [**9**].

Additionally, models of the electroencephalogram (EEG) and magnetoencephalogram (MEG) have been constructed and used for electromagnetic source analysis [**10**], for simulation of non-stationary EEG signals [**2**], for validation of event related synchronization–desynchronization estimation of alpha waves in EEG [**11**], for simulation of the spontaneous EEG [**12**], and as a description of the temporal stationarity in background noise seen in MEG

**Corresponding author: Electrical Engineering Department, Oregon Institute of Technology (Portland Campus), 20175 NW AmberGlen Ct, Suite 200, Beaverton, OR 97006, USA. email: daniel@metodlabs.com*

and EEG measurements [**13**]. Other uses of physiological signal models include interpretation of the Lempel–Ziv complexity [**14**], validation of a filter algorithm that corrects ectopic beats for heart-rate variability analysis [**15**], validation of spike detection in noisy neural recordings [**16**], validation of an ambulatory QRS detector [**17**], and comparison of noise sensitivity in multiple QRS detection algorithms [**18**]. A small sampling of other physiological signal models can be found in references [**19**] to [**22**].

One of the most important uses for a pressure signal model or simulator is validating commercially available pressure signal measurement devices. Synthetic generation of signals allows a huge and diverse variety of data to be rapidly generated that can be used to target and test both specific aspects and overall robustness of measurement devices. In many cases, accumulation of real physiological data that represent a wide variety of patient populations and conditions is prohibitively costly or impossible. Simulators are currently used in validation studies of commercially available devices such as oscillometric non-invasive blood pressure (NIBP) monitors. Numerous studies have been conducted using simulators to validate oscillometric NIBP monitors, to perform consistency comparisons using synthetic signals with and without artefacts [**23**], to look for systematic differences between monitors [**24**], and to compare repeatability and differences between monitors [**25**]. Several other studies have been published comparing oscillometric NIBP devices and reporting on commercially available simulators [**26–30**]. While there are currently several simulators commercially available to evaluate oscillometric NIBP devices, there are none that can be used to validate invasive pressure signal devices such as those that measure arterial blood pressure (ABP) and intracranial pressure (ICP).

Models for physiological pressure signals have also been extensively used in research for a variety of applications [**31–35**]. However, there are currently no journal publications describing invasive cardiovascular pressure signal models. In this paper a statistical model for cardiovascular pressure signals such as ABP and ICP that incorporates the effects of respiration on pressure signals and can be used to generate synthetic signals with time-domain and frequency-domain characteristics matching any desired subject population is described. The model can be used for development and validation of algorithms that operate on cardiovascular pressure signals and as a simulator for validating and comparing commercially available devices used for invasive pressure devices that measure signals such as ICP and ABP. The effectiveness of the model is demonstrated by comparing synthetic ICP signals generated with the proposed model with ICP real signals taken from pediatric patients with traumatic brain injury.

2 MODEL DESCRIPTION

Biomedical pressure signals possess a variety of different morphologies. The pulse morphology of the ABP and SpO2 signals is well known and consists of a systolic peak, dicrotic notch, and dicrotic peak. ICP has a similar pulse morphology, but often has a third peak. Common morphologies are demonstrated using two ICP signals in the time-domain and a frequency-domain example of pressure signals taken from pediatric patients with traumatic brain injury. In Fig. 1(a) a typical low-pressure morphology can be seen. In this signal, the various features including the percussion peak, dicrotic notch, and dicrotic peak are annotated. Specific features characteristic of a low-pressure signal include a well-defined dichrotic notch and lower peak pressure value compared with a high-pressure morphology as typified in Fig. 1(b). As seen in Fig. 1(b), the dicrotic notch is absent, the tidal peak appears, and the peak pressure is higher. Figure 3 (given later) demonstrates the frequency-domain characteristics common in pressure signals. The annotations highlight the typical frequency-domain characteristics that the proposed model will simulate.

2.1 Pressure signal model

Biomedical pressure signals can be modelled as a sum of N harmonically related sinusoidal signals modulated by respiration according to

$$x(t) = [1 - m(t)r_{\mathrm{n}}(t)] \sum_{k=1}^{N} \alpha_k(t) \cos\left[\theta_{\mathrm{c}_k}(t)\right] + r(t) + u(t) \quad (1)$$

where $r(t)$ is the additive component of the respiratory signal, $r_{\mathrm{n}}(t)$ is the normalized respiratory signal, $m(t)$ is the modulation index, $\{\alpha_k(t)\}_{k=1}^{N}$ are the scalar multipliers for each of the harmonic signal components, $\{\theta_{\mathrm{c}_k}(t)\}_{k=1}^{N}$ denote the angles corresponding to each of the harmonics, and $u(t)$ denotes coloured noise. The instantaneous cardiac frequency

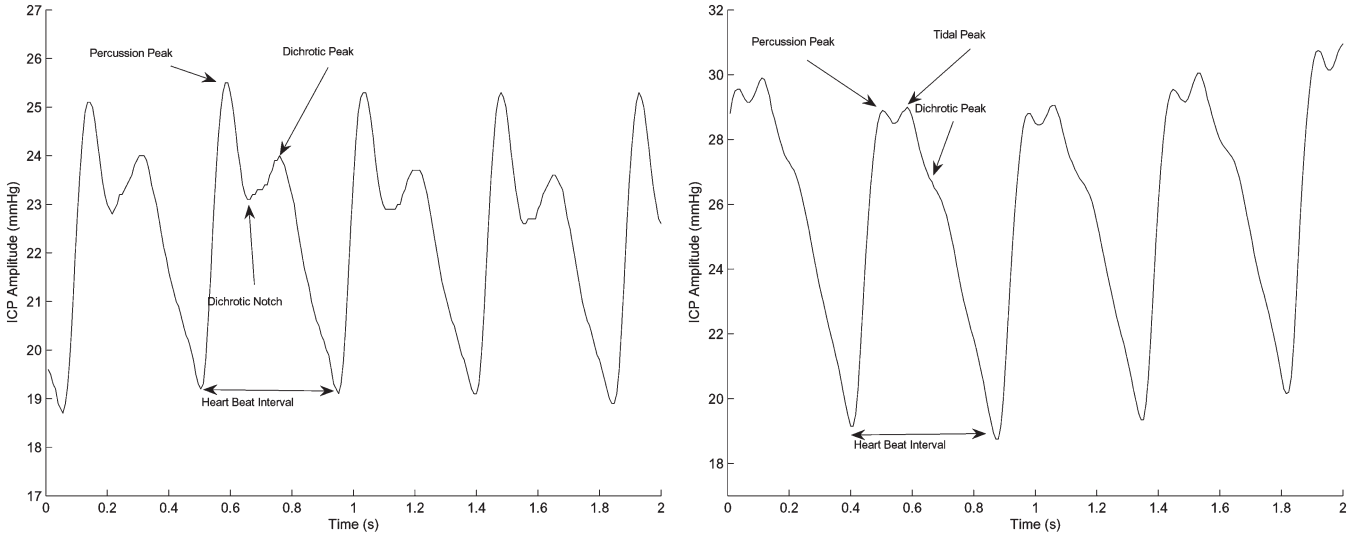

Fig. 1 Time-domain example of (a) a low-pressure and (b) a high-pressure ICP signal and taken from a pediatric patient with traumatic brain injury

f_{c_i} is given by

$$\frac{\mathrm{d}\theta_{c_k}(t)}{t} = 2\pi f_{c_i}(t) \tag{2}$$

where $f_{ci}(t)$ can be modelled as an autoregressive random process.

The normalized respiratory signal $r_n(t)$ can also be modelled as a sum of P harmonically related sinusoids, according to

$$r_n(t) = \sum_{k=1}^{P} \cos\left[\theta_{r_k}(t)\right] + v(t) \tag{3}$$

where $\left\{\theta_{r_k}(t)\right\}_{k=1}^{P}$ denotes the angles corresponding to the harmonics composing the respiratory signal, and $v(t)$ denotes coloured noise. The instantaneous respiratory frequency f_{r_i} is given by

$$\frac{\mathrm{d}\theta_{r_k}(t)}{t} = 2\pi f_{r_i}(t) \tag{4}$$

and can also be modelled as an autoregressive random process.

This model takes into account the frequency variability of the cardiac and respiratory components by modeling $\theta_{c_k}(t)$ and $\theta_{r_k}(t)$ as two correlated random processes with bandwidth β_c and β_r respectively. These bandwidths control the heart rate variability and the respiratory rate variability.

The model that is proposed in equation (1) is a generalization of previously published models. Note that if only the first two harmonics of the cardiac signal $\left\{\theta_{c_k}(t)\right\}_{k=1}^{2}$ are considered, if the respiratory signal is assumed to have a single harmonic $\theta_{r_k}(t)$, and the modulation index $m(t)$ is constant, i.e. $m(t)=m$, the model reduces to

$$x(t) = [1 - m r_n(t)] \sum_{k=1}^{2} \alpha_k \cos\left[\theta_{c_k}(t)\right] + r(t) + u(t) \tag{5}$$

for constant scalar multipliers, i.e. $\alpha_k(t)=\alpha_k$. This model can be further simplified if the heart rate variability is not accounted for and if it is assumed that the subject is being mechanically ventilated, resulting in a constant respiratory frequency given by

$$x(t) = a(t)[\alpha_1 \cos(2\pi f_c t) + \alpha_2 \cos(2\pi 2 f_c t) + \theta] + u(t) \tag{6}$$

where the cardiac frequency f_c is constant, the second harmonic has a phase shift with respect to the fundamental cardiac component θ, and the modulation signal $a(t)$ has a constant modulation index m and constant respiratory frequency f_r and is given by $a(t)=1-m\cos(2\pi f_r t)$.

2.2 Additive noise; baseline drift

The baseline drift artefact $b(t-\tau_b)$ is modelled as an additive effect on the pressure signal $x(t)$ according to

$$x_b(t) = x(t) + b(t - \tau_b) \tag{7}$$

where $b(t-\tau_b)$ is a step function starting at time τ_b and is given by

$$b(t-\tau_b)=\begin{cases}0, & t<\tau_b\\ k_b, & t>\tau_b\end{cases} \tag{8}$$

where τ_b is a continuous random variable drawn from a uniform distribution, $\tau_b \sim U\left(\mu_{\tau_b}, \sigma^2_{\tau_b}\right)$ with mean μ_{τ_b} and variance $\sigma^2_{\tau_b}$. Analogously, k_b is modelled as a continuous random variable drawn from a Gaussian distribution $k_b \sim f_b\left(\mu_b, \sigma^2_b\right)$ with user-specified mean μ_b and variance σ^2_b. This choice of random variable allows the user to simulate both increasing and decreasing baseline drift.

2.3 Impulse noise

Impulse noise can be caused by a variety of artefacts such as abrupt motion artefacts. Impulse artefacts $d_k(t-\tau_d)$ are modelled as an additive effect on the pressure signal $x(t)$, according to

$$x_d(t)=x(t)+\sum_{k=1}^{N} d_k(t-\tau_d) \tag{9}$$

where N, the number of impulse artefacts present in the signal, is a continuous random variable drawn from a Gaussian distribution $N \sim f_N\left(\mu_N, \sigma^2_N\right)$ with user-specified mean μ_N and variance σ^2_N, and $d_k(t-\tau_d)$ is an impulse function starting at time τ^k_d, according to

$$d_k(t-\tau_d)=\begin{cases}0, & t\neq\tau^k_d\\ \int_{\tau_d-\varepsilon}^{\tau_d+\varepsilon} d(t-\tau_d) & \mathrm{d}t=k^k_d\end{cases} \tag{10}$$

where τ^k_d is a continuous random variable drawn from a uniform distribution $\tau^k_d \sim U\left(\mu_{\tau^k_d}, \sigma^2_{\tau^k_d}\right)$ with mean $\mu_{\tau^k_d}$ and variance $\sigma^2_{\tau^k_d}$. Analogously k^k_d is modelled as a continuous random variable drawn from a Gaussian distribution $k^k_d \sim f^k_b\left(\mu^k_d, \sigma^{2^k}_d\right)$ with user-specified mean μ^k_d and variance $\sigma^{2^k}_d$.

2.4 Power line interference

Power line interference is modelled as an additive effect on the pressure signal $x(t)$ by a multiharmonic sinusoidal signal $p(t)$, according to

$$x_p(t)=x(t)+p(t) \tag{11}$$

The interference signal $p(t)$ is given by

$$p(t)=\sum_{k=0}^{P} A_k \cos(2\pi f_0 kt+\phi_k) \tag{12}$$

where f_0 corresponds to the line interference frequency and P is the number of harmonics. In this implementation, $P=3$ and f_0 are user-specified parameters (60 Hz in the USA).

3 RESULTS AND DISCUSSION

Table 1 lists the user-specified parameters available in the proposed model. Note that all the parameters have a clear clinical interpretation as listed in Table 1. With these parameters, synthetic signals from diverse subject populations can be generated including animals, adults, the elderly, and children. For example, when simulating the ICP pulse morphology of a critically ill child, the heart rate could be selected near 2 Hz. Using a nominal heart rate of 1 Hz would correspond to a healthy adult. Altering other parameters listed in Table 1 with *a-priori* information about various patient populations enables researchers to simulate data from other patient populations. The proposed model is demonstrated

Table 1 Summary of user-specified parameters available in the proposed model

User-specified parameter	Description of parameter
m	Pulse pressure variation or modulation index
f_c	Heart rate (Hz)
f_r	Respiratory rate (Hz)
r_n	Pulse pressure magnitude (mmHg)
μ_p	Mean pressure (d.c. offset)
ϕ_2	Phase of second sinusoidal signal
$d_k(t-\tau_d)$	Motion artefact due to patient movements
t	Length of signal (s)
f_s	Sampling frequency (Hz)
$p(t)$	Power line interference
$b(t-\tau_b)$	Baseline drift

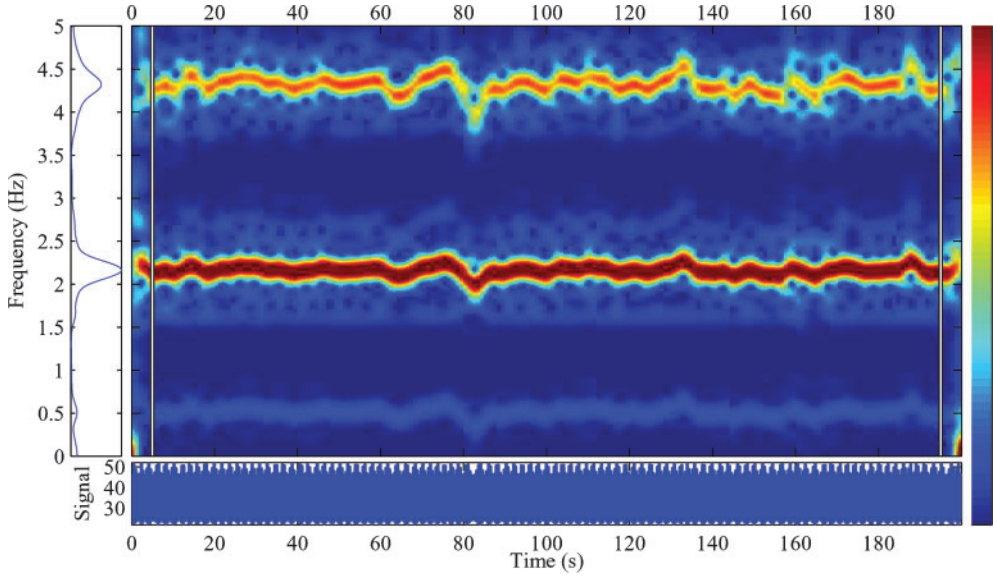

Fig. 2 Frequency-domain example of a synthetic ICP signal simulating a pediatric patient with traumatic brain injury

by comparing synthetic pressure signals generated by the proposed model against real ICP from pediatric patients in the time-domain. Noise-corrupted signals are not included for brevity of presentation. A frequency-domain synthetic signal is also presented in Fig. 2 and this was generated with the same patient parameters as the real signal shown in Fig 3.

Figure 4 shows examples of synthetic pressure signals generated with the proposed model with the objective of matching the pulse morphology of pediatric patients with traumatic brain injury. In these time-domain figures the dark-grey signal corresponds to the synthetic signal and the light grey signal represents the real pressure signals. Figure 4(a) shows a low-pressure ICP morphology. Note the well-defined dicrotic notch and lack of the tidal peak typical in low-pressure ICP morphologies. Figure 4(b) shows a high-pressure ICP morphology characterized by the absence of the dicrotic notch and the appearance of the tidal peak. Figure 2 is a frequency-domain representation of a synthetic ICP signal generated to match the frequency content of the signal shown in Fig. 3. Note how the model parameters can be user specified or automatically estimated to generate ensembles of synthetic signals

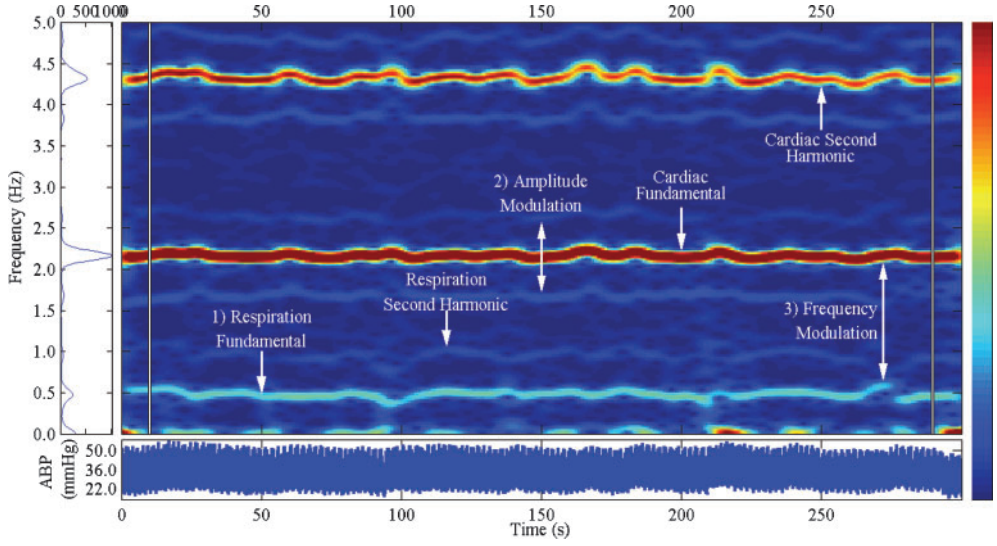

Fig. 3 Frequency-domain example of an ICP signal taken from a pediatric patient with traumatic brain injury

with time-domain and frequency-domain characteristics matching a wide range of patient populations or conditions. The ability to generate these ensembles is important for validation and assessment of algorithms and commercially available devices designed to operate on cardiovascular pressure signals.

Models for physiological pressure signals have been used in a variety of research applications. For instance, in reference [**31**] a synthetic ABP signal was used to validate a pulse pressure variation algorithm. The development of a Kalman filter approach to spectral estimation in non-stationary biomedical signals utilized both a model and a real ICP signal for comparison and validation [**32**]. Other studies have used synthetic ICP signals to validate and compare a brain pressure monitor and intracranial pressure transducers [**33**, **34**]. In reference [**35**], an approximate entropy interpretation study included synthetic ICP signals with a range of characteristics to analyse approximate entropy in the context of biomedical signal analysis. One disadvantage to these pressure signal models is that they are developed within the framework of a different goal, i.e. presenting a novel algorithm. Consequently, as much time and effort is spent developing a model for validation and comparison as is spent developing the algorithm or technique that the researcher presents.

In an effort to address this issue in the context of cardiovascular pressure signals, in this paper a statistical model and simulator for cardiovascular pressure signals including three noise sources commonly found in ABP and ICP patient data are described. The model incorporates the additive, amplitude modulation, and frequency modulation effects of respiration on pressure signals. Additionally, it accounts for the heart-rate variability typically present in healthy or sick individuals. The user-specified parameters of the model all have a clear clinical interpretation such as mean heart rate, respiratory frequency, heart-rate variability, mean pressure, pulse pressure, and pulse pressure variation. It was demonstrated that this model produces synthetic pressure signals having the same time-domain and frequency-domain morphologies as real cardiovascular pressure signals. Additionally, owing to the number of user-specified parameters, the proposed model is general enough to simulate pressure signals from many different patient populations including children, adults, and animals.

4 SUMMARY

A statistical model and simulator for cardiovascular pressure signals and noise have been described. The model can be used to synthesize ensembles of invasive pressure signals designed to match real pressure signals from specific subject populations by adjusting the user-specified parameters of the model. The user-specified parameters of the model have clear clinical interpretations such as the mean heart rate, mean breathing frequency, heart-rate variability, mean pressure, pulse pressure, and pulse pressure variation. This model can be used for validation of commercially available invasive pressure monitors and for assessment and validation of

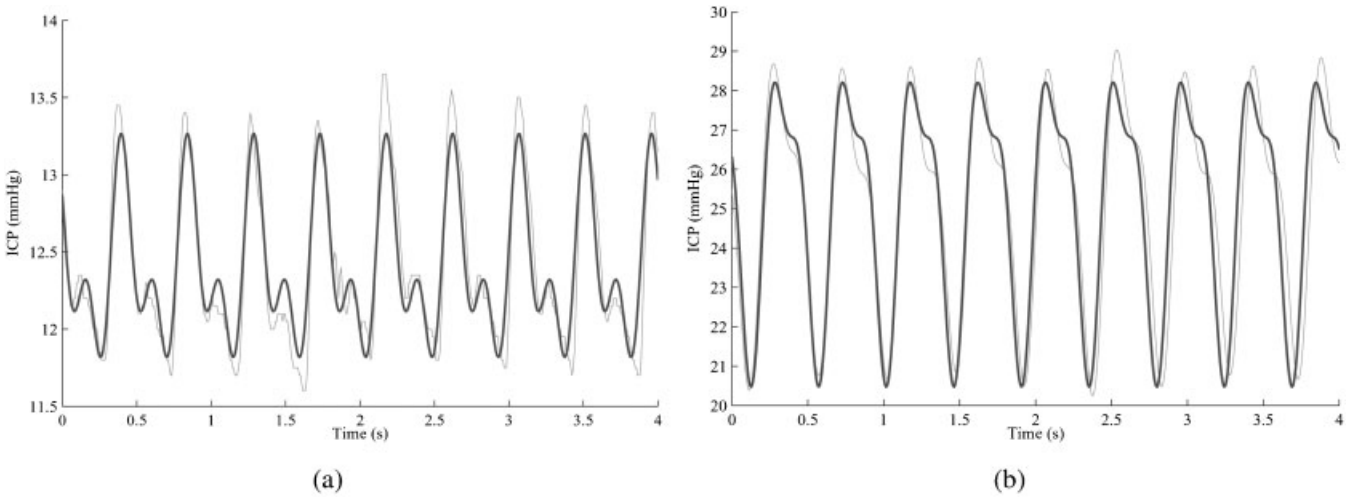

Fig. 4 Comparison of (a) one low-pressure synthetic signal and (b) one high-pressure synthetic signal generated by the proposed model (dark-grey curves) against real ICP signals (light-grey curves) taken from pediatric patients with traumatic brain injury

biomedical signal-processing algorithms designed to estimate any of these parameters.

REFERENCES

1 **Duchêne, J.** and **Hogrel, J. Y.** A model of EMG generation. *IEEE Trans. Biomed. Engng*, 2000, **47**(2), 192–201.

2 **Kaipio, J. P.** and **Karjalainen, P. A.** Simulation of nonstationary EEG. *Biol. Cybernetics*, 1997, **76**(5), 349–356.

3 **Nakamura, M.** Waveform estimation from noisy signals with variable signal delay using bispectrum averaging. *IEEE Trans. Biomed. Engng*, 1993, **40**(2), 118–127.

4 **Kim, S.** and **McNames, J.** Tracking tremor frequency in spike trains using the extended Kalman smoother. *IEEE Trans. Biomed. Engng*, 2006, **53**(8), 1569–1577.

5 **Aboy, M.** and **Falkenberg, J. H.** An automatic algorithm for stationary segmentation of extracellular microelectrode recordings. *Med. Biol. Engng Computing*, 2006, **44**(6), 511–515.

6 **Merletti, R., Roy, S. H., Kupa, E., Roatta, S.,** and **Granata, A.** Modeling of surface myoelectric signals – part II: model-based signal interpretation. *IEEE Trans. Biomed. Engng*, 1999, **46**(7), 821–829.

7 **Farina, D., Merletti, R., Indino, B.,** and **Graven-Nielsen, T.** Surface EMG crosstalk evaluated from experimental recordings and simulated signals. Reflections on crosstalk interpretation, quantification and reduction. *Meth. Inf. Medicine*, 2004, **43**(1), 30–35.

8 **Fuglevand, A. J., Winter, D. A., Patla, A. E.,** and **Stashuk, D.** Dectection of motor unit action potentials with surface electrodes: influence of electrode size and spacing. *Biol. Cybernetics*, 1992, **67**(2), 143–153.

9 **Lowery, M. M., Stoykov, N. S., Dewald, J. P. A.,** and **Kuiken, T. A.** Volume conduction in an anatomically based surface EMG model. *IEEE Trans. Biomed. Engng*, 2004, **51**(12), 2138–2147.

10 **Waldorp, L. J., Huizenga, H. M., Grasman, R. P. P. P., Böcker, K. B. E., de Munck, J. C.,** and **Molenaar, P. C. M.** Model selection in electromagnetic source analysis with an application to VEFs. *IEEE Trans. Biomed. Engng*, 2002, **49**(10), 1121–1129.

11 **Kaipio, J. P.** and **Karjalainen, P. A.** Estimation of event-related synchronization changes by a new TVAR method. *IEEE Trans. Biomed. Engng*, 1997, **44**(8), 649–656.

12 **Bai, O., Nakamura, M., Ikeda, A.,** and **Shibasaki, H.** Nonlinear Markov process amplitude EEG model for nonlinear coupling interaction of spontaneous EEG. *IEEE Trans. Biomed. Engng*, 2000, **47**(9), 1141–1146.

13 **Bijma, F., de Munck, J. C., Huizenga, H. M.,** and **Hecthaar, R. M.** A mathematical approach to the temporal stationarity of background noise in MEG/EEG measurements. *Neuroimage*, 2003, **20**(1), 233–243.

14 **Aboy, M., Hornero, R., Abásolo, D.,** and **Alvarez, D.** Interpretation of the Lempel–Ziv complexity measure in the context of biomedical signal analysis. *IEEE Trans. Biomed. Engng*, 2006, **53**(11), 2282–2288.

15 **Storck, N., Ericson, M., Lindblad, L.,** and **Jensen-Urstad, M.** Automatic computerized analysis of heart rate variability with digital filtering of ectopic beats. *Clin. Physiology*, 2001, **21**(1), 115–24.

16 **Nenadic, Z.** and **Burdick, J. W.** Spike detection using the continuous wavelet transform. *IEEE Trans. Biomed. Engng*, 2005, **52**(1), 74–87.

17 **Ruha, A., Sallinen, S.,** and **Nissilä, S.** A real-time microprocessor QRS detector system with a 1-ms timing accuracy for the measurement of ambulatory HRV. *IEEE Trans. Biomed. Engng*, 1997, **44**(3), 159–167.

18 **Friesen, G. M., Jannett, T. C., Jadallah, M. A., Yates, S. L., Quint, S. R.,** and **Nagle, H. T.** A comparision of the noise sensitivity of nine QRS detection algorithms. *IEEE Trans. Biomed. Engng*, 1990, **37**(1), 85–98.

19 **Feng, L., Siu, K., Moore, L. C., Marsh, D. J.,** and **Chon, K. H.** A robust method for detection of linear and nonlinear interactions: application to renal blood flow dynamics. *Ann. Biomed. Engng*, 2006, **34**(2), 339–353.

20 **Goldman, J. M., Ward, D. R.,** and **Daniel, L.** BreathSim, a mathematical model-based simulation of the anesthesia breathing circuit, may facilitate testing and evaluation of respiratory gas monitoring equipment. *Biomed. Sci. Instrumn*, 1996, **32**, 293–298.

21 **Gootzen, T. H., Stegeman, D. F.,** and **Van Oosterom, A.** Finite limb dimensions and finite muscle length in a model for the generation of electromyographic signals. *Electroencephalography Clin. Neurophysiology*, 1991, **81**(2), 152–162.

22 **Vai, M. I.** and **Zhou, L. G.** Beat-to-beat ECG ventricular late potentials variance detection by filter bank and wavelet transform as beat-sequence filter. *IEEE Trans. Biomed. Engng*, 2004, **51**(8), 1407–1413.

23 **Amoore, J. N.** A simulation study of the consistency of oscillometric blood pressure measurements with and without artefacts. *Blood Pressure Monitoring*, 2000, **5**(2), 69–79.

24 **Amoore, J. N.** and **Scot, D. H.** Can simulators evaluate systematic differences between oscillometric non-invasive blood-pressure monitors? *Blood Pressure Monitoring*, 2000, **5**(2), 81–89.

25 **Sims, A. J., Reay, C. A., Bousfield, D. R., Menes, J. A.,** and **Murray, A.** Oscillometric blood pressure devices and simulators: measurements of repeatability and differences between models. *J. Med. Engng Technol.*, 2005, **29**(3), 112–118.

26 **Murray, I. C., Amoore, J. N.,** and **Scott, D. H. T.** Differences in oscillometric non-invasive blood pressure measurements recorded by different revisions of the Philips component monitoring system. *Blood Pressure Monitoring*, 2005, **10**(4), 215–222.

27 **Amoore, J. N., Vacher, E., Murray, I. C., Mieke, S., King, S. T., Smith, F. E.,** and **Murray, A.** Can a simulator that regenerates physiological waveforms evaluate oscillometric non-invasive blood pressure devices? *Blood Pressure Monitoring*, 2006, **11**(2), 63–67.

28 **Amoore, J. N.** and **Geake, W. B.** An evaluation of three oscillometric non-invasive blood pressure simulators. *J. Clin. Engng*, 1997, **22**(2), 93–100.

29 **Ng, K. G.** and **Small, C. F.** Review of methods & simulators for evaluation of noninvasive blood pressure monitors. *J. Clin. Engng*, 1992, **17**(6), 469–479.

30 **Ng, K. G.** and **Small, C. F.** Update on methods & simulators for evaluation of noninvasive blood pressure monitors. *J. Clin. Engng*, 1994, **19**(2), 125–134.

31 **Aboy, M., McNames, J., Thong, T., Phillips, C. R., Ellenby, M. S.,** and **Goldstein, B.** A novel algorithm to estimate the pulse pressure variation index deltaPP. *IEEE Trans. Biomed. Engng*, 2004, **51**(12), 2198–2203.

32 **Aboy, M., Márquez, O. W., McNames, J., Hornero, R., Trong, T.,** and **Goldstein, B.** Adaptive modeling and spectral estimation of nonstationary biomedical signals based on Kalman filtering. *IEEE Trans. Biomed. Engng*, 2005, **52**(8), 1485–1489.

33 **Czosnyka, M., Czosnyka, Z.,** and **Pickard, J. D.** Laboratory testing of three intracranial pressure microtransducers: technical report. *Neurosurgery*, 1996, **38**(1), 219–224.

34 **Czosnyka, M., Czosnyka, Z.,** and **Pickard, J. D.** Laboratory testing of the Spiegelberg brain pressure monitor: a technical report. *J. Neurology, Neurosurg. Psychiatry*, 1997, **63**(6), 732–735.

35 **Hornero, R., Aboy, M., Abásolo, D., McNames, J.,** and **Goldstein, B.** Interpretation of approximate entropy: analysis of intracranial pressure approximate entropy during acute intracranial hypertension. *IEEE Trans. Biomed. Engng*, 2005, **52**(10), 1671–1680.